

13

LEVEL II

12

DNA 5284F

**INVESTIGATION OF THE COMPUTER MODELING
OF THE DIRECT COUPLING OF HIGH
EXPLOSIVE ENERGY TO THE GROUND FOR
SURFACE TANGENT-ABOVE TNT SPHERES
(100-500 TONS)**

Jeffrey M. Thomsen
Physics International Company
2700 Merced Street
San Leandro, California 94577

DTIC
1980
E

7 April 1980

Final Report for Period 29 May 1979-31 March 1980

CONTRACT No. DNA 001-79-C-0358

APPROVED FOR PUBLIC RELEASE;
DISTRIBUTION UNLIMITED.

THIS WORK SPONSORED BY THE DEFENSE NUCLEAR AGENCY
UNDER RDT&E RMSS CODE B344079464 Y99QAXSA00224 H2590D.

Prepared for
Director
DEFENSE NUCLEAR AGENCY
Washington, D. C. 20305

80 12 31 82

AD A 092537

DDC FILE COPY

Destroy this report when it is no longer
needed. Do not return to sender.

PLEASE NOTIFY THE DEFENSE NUCLEAR AGENCY,
ATTN: STTI, WASHINGTON, D.C. 20305, IF
YOUR ADDRESS IS INCORRECT, IF YOU WISH TO
BE DELETED FROM THE DISTRIBUTION LIST, OR
IF THE ADDRESSEE IS NO LONGER EMPLOYED BY
YOUR ORGANIZATION.



UNCLASSIFIED

SECURITY CLASSIFICATION OF THIS PAGE (When Data Entered)

19) REPORT DOCUMENTATION PAGE		READ INSTRUCTIONS BEFORE COMPLETING FORM
1. REPORT NUMBER 18) DNA 5284F	2. GOVT ACCESSION NO. AD-A093	3. RECIPIENT'S CATALOG NUMBER 537
4. TITLE (and Subtitle) INVESTIGATION OF THE COMPUTER MODELING OF THE DIRECT COUPLING OF HIGH EXPLOSIVE ENERGY TO THE GROUND FOR SURFACE TANGENT—ABOVE TNT SPHERES (100-500 TONS).	5. TYPE OF REPORT & PERIOD COVERED 9) Final Report, for Period 29 May 79—31 Mar 80	6. PERFORMING ORG. REPORT NUMBER 14) PIFR-1306
7. AUTHOR 10) Jeffrey M. Thomsen	8. CONTRACT OR GRANT NUMBER(s) 15) DNA 001-79-C-0358	
9. PERFORMING ORGANIZATION NAME AND ADDRESS Physics International Company 2700 Merced Street San Leandro, California 94577	10. PROGRAM ELEMENT PROJECT, TASK AREA & WORK UNIT NUMBERS 17) A003 1) Subtask Y99QAXSA002-24	
11. CONTROLLING OFFICE NAME AND ADDRESS Director Defense Nuclear Agency Washington, D.C. 20305	12. REPORT DATE 11) 7 April 1980	13. NUMBER OF PAGES 48
14. MONITORING AGENCY NAME & ADDRESS (if different from Controlling Office)	15. SECURITY CLASS (of this report) UNCLASSIFIED	15a. DECLASSIFICATION DOWNGRADING SCHEDULE N/A
16. DISTRIBUTION STATEMENT (of this Report) Approved for public release; distribution unlimited.		
17. DISTRIBUTION STATEMENT (of the abstract entered in Block 20, if different from Report)		
18. SUPPLEMENTARY NOTES This work sponsored by the Defense Nuclear Agency under RDT&E RMSS Code B344079464 Y99QAXSA00224 H2590D.		
19. KEY WORDS (Continue on reverse side if necessary and identify by block number) High Explosive Cratering Direct Coupling Middle Gust III Cratering Calculations		
20. ABSTRACT (Continue on reverse side if necessary and identify by block number) The calculational modeling of the initial coupling of impulse and energy to the ground for large yield (100-500 tons) surface tangent-above spherical TNT cratering calculations was investigated. A pressure-time surface boundary condition was found to be an accurate way of modeling this initial coupling, if the styrofoam/plywood structure supporting the TNT charge is neglected. The specific boundary condition used by California Research and Technology, Inc., in its current baseline Middle Gust III calculation was examined, and		

UNCLASSIFIED

SECURITY CLASSIFICATION OF THIS PAGE (When Data Entered)

20. ABSTRACT (Continued)

compared favorably with ones previously used. No cratering calculations were found which adequately modeled the TNT charge support structure. One-dimensional calculations were performed to assess its effect on the initial coupling. Results showed that inclusion of a reasonable model for the support structure in a two-dimensional cratering calculation would cause higher close-in peak pressures in the soil, while probably not changing the total directly coupled energy or impulse significantly. Two-dimensional effects would predominate in such a calculation, however, and these were not addressed in the present investigation.

A

UNCLASSIFIED

SECURITY CLASSIFICATION OF THIS PAGE (When Data Entered)

PREFACE

The author would like to thank Dr. Robert Port and Mr. John Lewis of R and D Associates for their help and encouragement throughout this investigation, and also Mr. Steve Melzer of Civil Systems, Inc., and Mr. Sheldon Schuster of California Research and Technology, Inc., for many useful technical discussions. Finally, the author would like to acknowledge the efforts of Mr. Peter Dzwilewski of Civil Systems, Inc., in providing much unpublished data from past cratering calculations.

During this program, Major Robert Swedock, USA, was the DNA Contracting Officer's representative; Dr. Eugene Sevin was the Chief of the DNA Strategic Structures Division.

Accession For	
NTIS GRA&I	<input checked="" type="checkbox"/>
DDC TAB	<input type="checkbox"/>
Unannounced	<input type="checkbox"/>
Justification	<input type="checkbox"/>
By _____	
Date _____	
Special Agent Grades	
Special Agent Lead/er	
Disc. Serial	
A	

TABLE OF CONTENTS

	<u>Page</u>
PREFACE.....	1
LIST OF ILLUSTRATIONS.....	3
SECTION 1 INTRODUCTION.....	5
SECTION 2 MATERIAL MODELING FOR THE CALCULATIONS.....	9
2.1 High Explosive (TNT).....	9
2.2 Soil.....	12
2.3 Styrofoam, Plywood and Air.....	14
SECTION 3 CALCULATIONAL RESULTS AND ANALYSES.....	19
3.1 Conditions Within a 100 Ton TNT Sphere.....	19
3.2 Modeling of the Air-Ground Interface.....	24
3.3 Effect of the Charge Support Structure.....	30
SECTION 4 CONCLUSIONS.....	38
REFERENCES	40

LIST OF ILLUSTRATIONS

<u>Figure</u>		<u>Page</u>
1.1	Explosive charge's upper hemisphere, Middle Gust III.....	6
2.1	Comparison of isentropes describing the expansion of TNT using the JWL and LSZK equations of state.....	11
2.2	Middle Gust III soil model hydrostat.....	13
2.3	Dependence of theoretical styrofoam Hugoniots on initial volume.....	15
2.4	Styrofoam Hugoniots at initial density = 0.055 g/cc.....	16
2.5	Styrofoam Hugoniots at initial density = 0.018 g/cc.....	17
3.1	Pressure versus radius within a 100 ton sphere at a time all the explosive has detonated.....	20
3.2	Specific internal energy vs. radius within a 100 ton TNT sphere at the time all the explosive has detonated.....	21
3.3	Density vs. radius within a 100 ton TNT sphere at the time all the explosive has detonated.....	22
3.4	Particle velocity vs. radius within a 100 ton TNT sphere at the time all the explosive has detonated.....	23
3.5	Pressure histories at the edge of a 100 ton TNT sphere from 1D calculations.....	25
3.6	Percent of yield coupled to the ground versus time for Mixed Company event and the Middle Gust III event.....	31

<u>Figure</u>		<u>Page</u>
3.7	Comparison of close-in total impulse delivered to the ground by 100 ton surface tangent-above TNT spheres.....	32
3.8	Pressure histories at the soil interface.....	34
3.9	Specific impulse at the soil interface.....	35
3.10	Pressure histories at 0.5 m (1.6 ft) depth in the soil.....	36

SECTION 1

INTRODUCTION

The Middle Gust III baseline calculation, to be performed by California Research and Technology (CRT), Inc., will use a pressure-time boundary condition to describe the surface loading (References 1 and 2). The close-in [0-3 m (0-10 ft) radius] pressure-time fit will be made to a recent Air Force Weapons Laboratory (AFWL) calculation of the airblast from a 100 ton TNT sphere (References 2 and 3). Beyond 3 m (10 ft), the pressure-time boundary condition will fit the averaged Middle Gust III airblast data (Reference 3). The actual fit used in the calculation was developed by Schuster of CRT, and is currently being used in several coarsely zoned preliminary calculations which are being performed in advance of the baseline calculation.

Since most of the energy (at least 80 percent) that produces the final crater comes from the energy coupled over the dimensions of approximately the high explosive (HE) charge diameter [4.9 m (16 ft)], it is appropriate to investigate and review the details of the calculational modeling that led to the pressure-time boundary condition being used in that region. In particular, it is important to compare the assumptions made by the AFWL in modeling the HE source with the actual Middle Gust III charge geometry. The as-built Middle Gust III TNT source is shown in Figure 1.1 (Reference 4). The 100 ton surface-tangent TNT sphere was constructed by stacking 17 kg (37.6 lb) rectangular TNT blocks. The TNT support structure consisted of two 4.9 m (16 ft) diameter sheets of 19 mm (3/4 inch) thick plywood, upon which were stacked a low density charge support material called Phurane.* This material has a density of 0.032 g/cm³ (2 lbs/ft³) and was cut from sheets to approximate the outline of the TNT charge to be stacked within it (Reference 5).

*Manufactured by Dow Chemical, Inc.

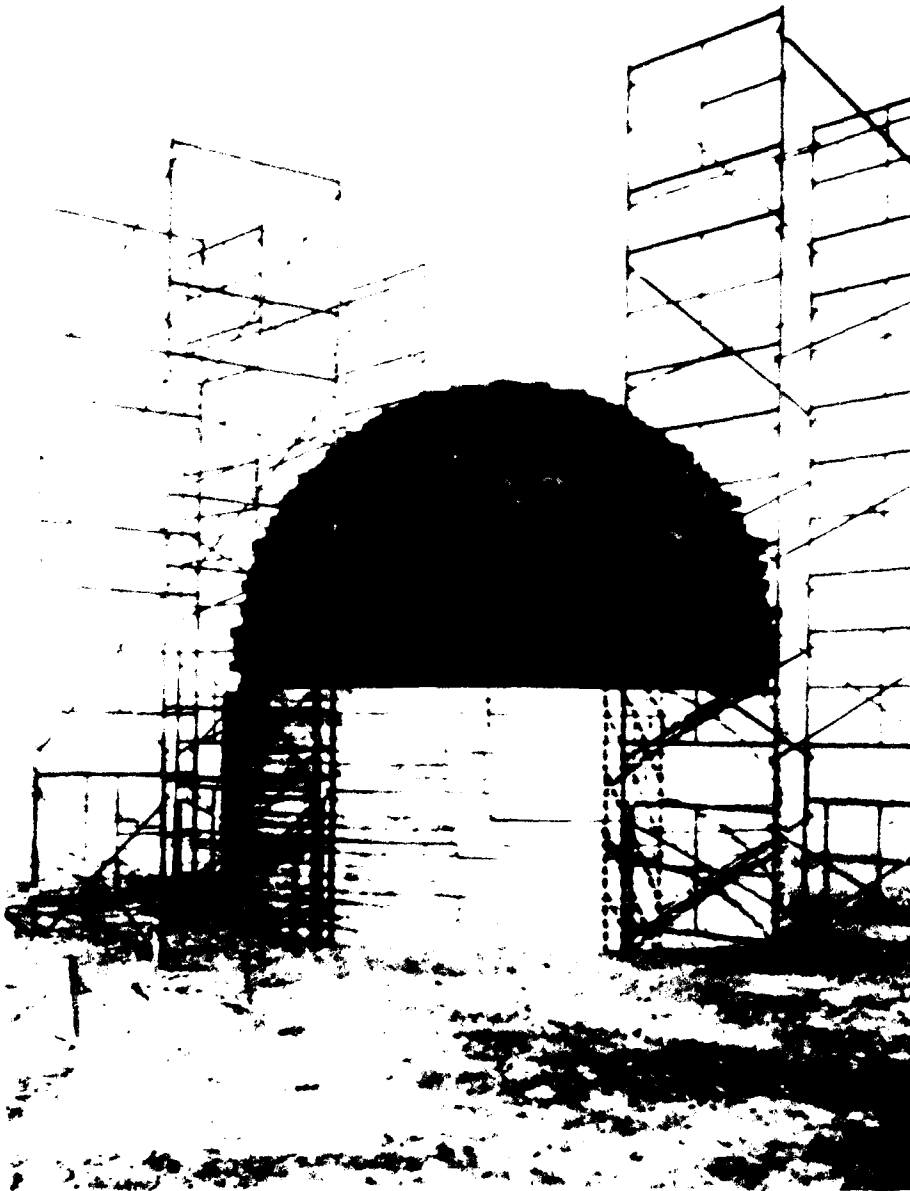


Figure 1.1 Explosive charge's upper hemisphere,
Middle Gust III.

The charge support extended to approximately one charge radius above the ground surface.

The AFWL recalculation of a 100 ton TNT sphere (referred to in this report as the "new calculation"), from which the pressure-time boundary within a 3 m (10 ft) radius of the ground zero is being obtained, is currently unpublished. Some of the details of this calculation were obtained from Dr. Needham (currently of Systems Science and Software, Inc.) and Lt. Guise (AFWL/DYT). The Hull (Eulerian) calculation was performed for a spherical charge of TNT placed above, and tangent to a rigid (reflecting) boundary. The pressure versus time and maximum positive phase impulse were given for ranges of 0, 0.6, 1.2, 2.7, and 3.0 m (0, 2, 4, 7, and 10 ft). As well as including a reflecting boundary below the charge instead of Middle Gust soil, the calculation ignored the charge support structure; this region was filled with normal density air. The TNT sphere was not detonated in this calculation; the calculation was begun at the time the detonation wave reached the boundary of the sphere (240.5 cm). The conditions within the sphere, including pressure, density, internal energy, and radial velocity, were obtained from a similarity solution of the detonation of a 100 ton TNT sphere performed by Nawrocki (Reference 6). The TNT detonation conditions, which will be referred to in this report as the AFWL STD, were obtained in the early 1960's. They used an equation of state called Landau, Stanyukovich, Zeldovich, and Kompaneets (LSZK). This equation of state is an empirical fit to a strong blast wave solution for TNT during both the pre- and post-detonation phases.

Based on examination of the AFWL 100 ton recalculation, three specific items were investigated. The first of these was the effect of using more recently developed high-explosive equations of state to describe the HE detonation and the detonation products. The second point was the effect of replacing the rigid boundary with a movable soil boundary. The third point was the effect of including the charge support

structure in the two-dimensional calculation. Each of these points will be addressed in this report. The effect on the overall energy coupling results of including each of these three items in a "full-up" two-dimensional calculation will be estimated (based on one-dimensional calculations and a review of what other calculators have done).

SECTION 2

MATERIAL MODELING FOR THE CALCULATIONS

One-dimensional calculations were used as part of the investigation to aid the analysis efforts. To perform the calculations material models were required for TNT, Middle Gust III soil, styrofoam, plywood and air. This section describes the models used for these materials.

2.1 HIGH EXPLOSIVE (TNT)

To describe the 100 ton TNT spherical charge, two models are currently used. The first is the Landau, Stanyukovich, Zeldovich, and Kompaneets (LSZK) equation of state (EOS). This EOS is a standard model in the present AFWL HULL two-dimensional computer code, and in older AFWL codes, which might be considered to be forerunners of HULL, such as SHELL-OIL and SHELL-2 (Reference 6). The basic functional form, given in Reference 7, describes the state of the explosion products of a condensed explosive. Data from Lutsky (Reference 8) was used to derive the values of the constants required by the functional form to describe TNT. The resulting EOS is given (Reference 7) as:

$$P = 0.34 I \rho + 1877 \rho^{2.78} \quad (2.1)$$

where ρ is the density (Mg/m^3), I is the specific internal energy (J/g), and P is the pressure (MPa). This EOS was used by Nawrocki (Reference 6) to develop a similarity solution for the conditions within a completely burned 100 ton TNT sphere, at the time the detonation wave just reaches the edge of the sphere (radius = 2.405 m). This solution has been used as an initial condition in many subsequent airblast and cratering calculations.

Explosive initial conditions for the LSZK TNT model
(Reference 7) are:

TNT initial density:	1.56 Mg/m ³ (1.56 g/cm ³)
TNT detonation velocity:	6.81 m/ms (0.681 cm/ μ s)
TNT energy release:	4.264 X 10 ³ J/g (4.264 X 10 ¹⁰ ergs/g).

The total energy contained within a LSZK 100 ton TNT sphere is then 3.876 X 10¹¹ J; the total explosive mass is 9.09 X 10⁴ kg.

The second EOS currently in use is the Jones-Wilkins-Lee (JWL) EOS (Reference 9). This EOS describes the state of the explosion products for a wide range of explosives, including TNT. The JWL EOS form is widely accepted, and will not be described again here, as it is very well described in Reference 9. The TNT coefficients used are given in Table 2.1. The total energy contained within a 100 ton JWL TNT sphere is then 4.05 X 10¹¹ J or 4.6 percent more than in the LSZK treatment.

Table 2.1 JWL EOS coefficients for TNT.

A =	3.712
B =	0.0323
C =	0.0104527
R ₁ =	4.15
R ₂ =	0.95
ω =	0.30
E ₀ =	4.46 X 10 ³ J/g (0.07 Mbar-cm ³ /cm ³)
ρ_0 =	1.56 Mg/m ³ (1.56 g/cm ³)
D =	6.93 m/ms (0.693 cm/s)

It is useful to compare the isentropes produced by the LSZK and JWL forms for TNT. Such a comparison is given in Figure 2.1; the LSZK pressures are generally lower when the specific volume,

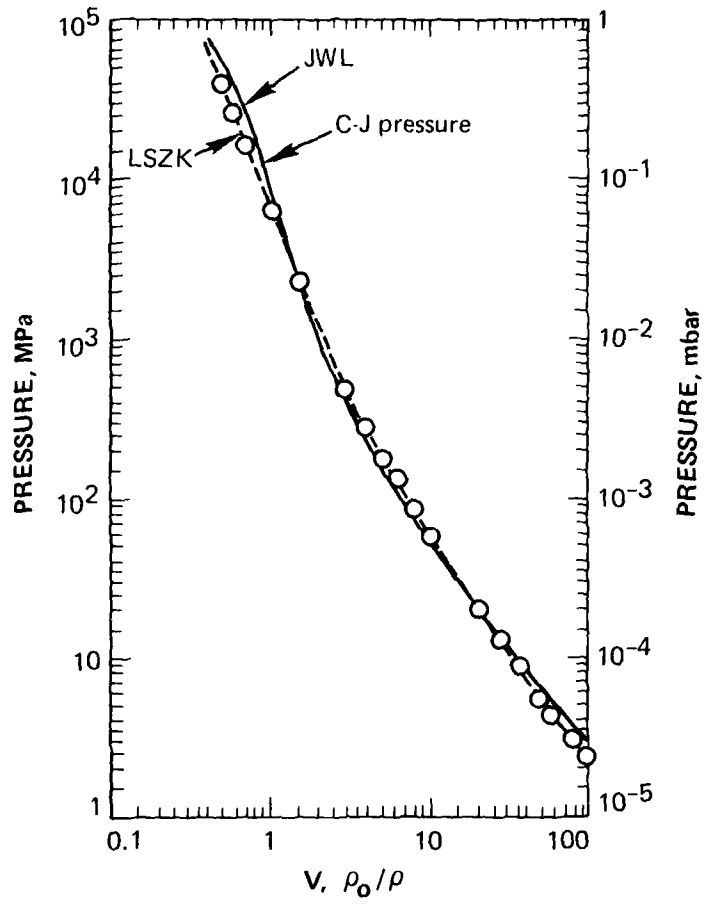


Figure 2.1 Comparison of isentropes describing the expansion of TNT using the JWL and LSZK equations of state.

V exceeds 1 ($V = \rho_0/\rho$ where ρ_0 is the initial density and ρ is the current density). This is the high pressure region [$P > 10$ GPa (100 kbar); the Chapman-Jouguet (C-J) pressure is 200 kbar]. For lower pressures, there are minor differences between the two curves. For $V > 20$, the LSZK curve falls below the JWL curve because of the lower value of gamma used ($\gamma = 1.30$ for JWL; 1.34 for LSZK).

2.2 SCIL

The Middle Gust III upper soil layers (0-2.7 m, 0-9 ft) are described by Zelasko (Reference 10) as a partly saturated sandy clay soil. For the investigation reported here, it was unnecessary to use the complete soil model describing this layer; a simpler one describing a 95 percent saturated, low strength soil using a initial density of approximately 2.1 g/cm^3 was considered sufficient. The basic reason was that only the initial phase of the charge coupling was to be investigated using one-dimensional calculations, and all that was required was an approximate soil boundary for the parametric studies.

The soil model was obtained from Reference 11, it describes 95 percent saturated, low strength sand/clay soil with a bulk density of 2.1 g/cm^3 and a grain density of 2.67 g/cm^3 . Figure 2.2 plots pressure versus compressibility, μ ($\mu = \rho/\rho_0 - 1$) over the pressure range of interest [$10 \leq P \leq 2 \times 10^4$ MPa (0.1 P 200 kbar)]. Pressure versus μ is given by:

$$P \text{ (MPa)} = 10\mu + 10^5\mu^2 \quad . \quad (2.2)$$

Thus the soil is highly compressible at low pressures, but becomes increasingly "stiff" with pressure. The unloading and loading curves are the same for this soil over the range of interest. A Poisson's ratio of 0.48 was used, and the initial sound speed in the soil was 0.70 m/s. A Mohr-Coulomb strength model was used, with a maximum value of Y ($Y = \sqrt{J_2}$) of 350 kPa (3.5 bar).

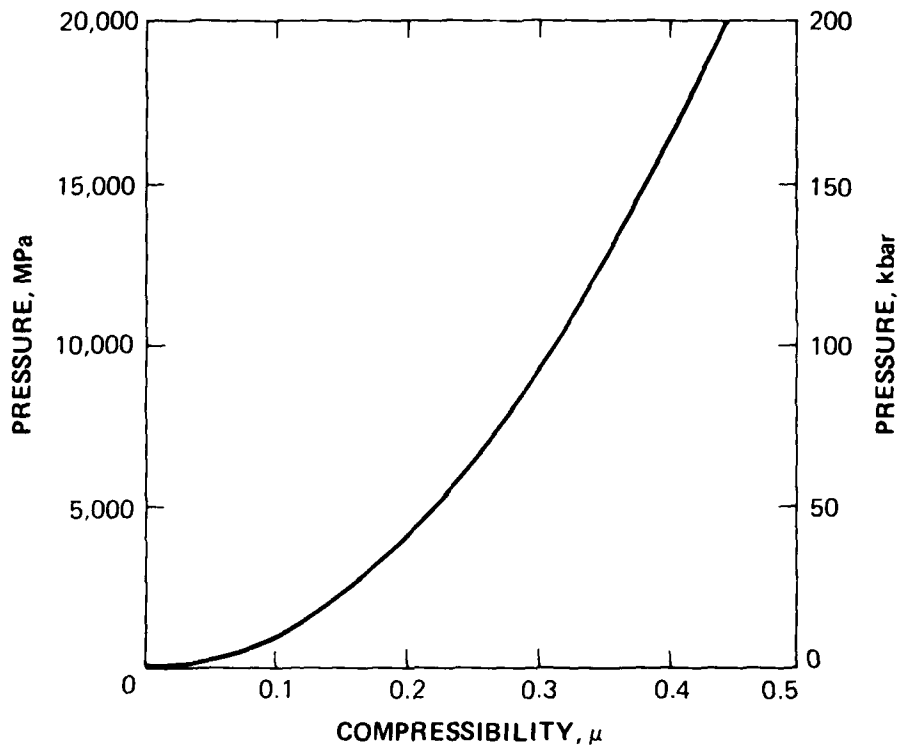


Figure 2.2 Middle Gust III soil model hydrostat.

2.3 STYROFOAM, PLYWOOD AND AIR

The Middle Gust III charge support structure was modeled using an EOS for styrofoam developed by F. H. Ree of Lawrence Livermore Laboratory (Reference 12). Hugoniot are shown in Figure 2.3 for various densities; the ones of greatest interest are 5 ($\rho_0 = 0.055 \text{ g/cm}^3$) and 6 ($\rho_0 = 0.018 \text{ g/cm}^3$). The initial density of the Middle Gust III charge support structure was 0.032 g/cm^3 . It is seen from Figure 2.3 that at these low densities shock heating effects become important, and the material begins to offer some resistance to total compaction (the solid density of the styrofoam is 1.044 g/cm^3). Many comparisons with LASL Hugoniot data are included in Reference 12. Two such comparisons are given in Figures 2.4 and 2.5. It must be noted that at the lowest density (0.018 g/cm^3 , Figure 2.5) the data show a great deal of scatter, and that the model does not fit the data very well. Agreement between model and data is much better in Figure 2.4 ($\rho_0 = 0.055 \text{ g/cm}^3$).

Plywood typically consists of thin Douglas fir sheets held together with an epoxy glue. A small piece of three-quarter-inch, grade A exterior plywood was obtained, and its density determined to be 0.54 g/cm^3 .

Hugoniot EOS data do not currently exist for plywood; however, data exist for a Douglas fir with an average density of 0.536 g/cm^3 (Reference 13). A linear fit to the Hugoniot data gives

$$U_s = 0.041 + 1.389 U_p \quad , \quad (2.3)$$

where U_s is the shock velocity ($\text{cm}/\mu\text{s}$) and U_p is the particle velocity ($\text{cm}/\mu\text{s}$). Using the classical Hugoniot relationships one can derive from Equation 2.3 the relationship between pressure, P and the density, ρ :

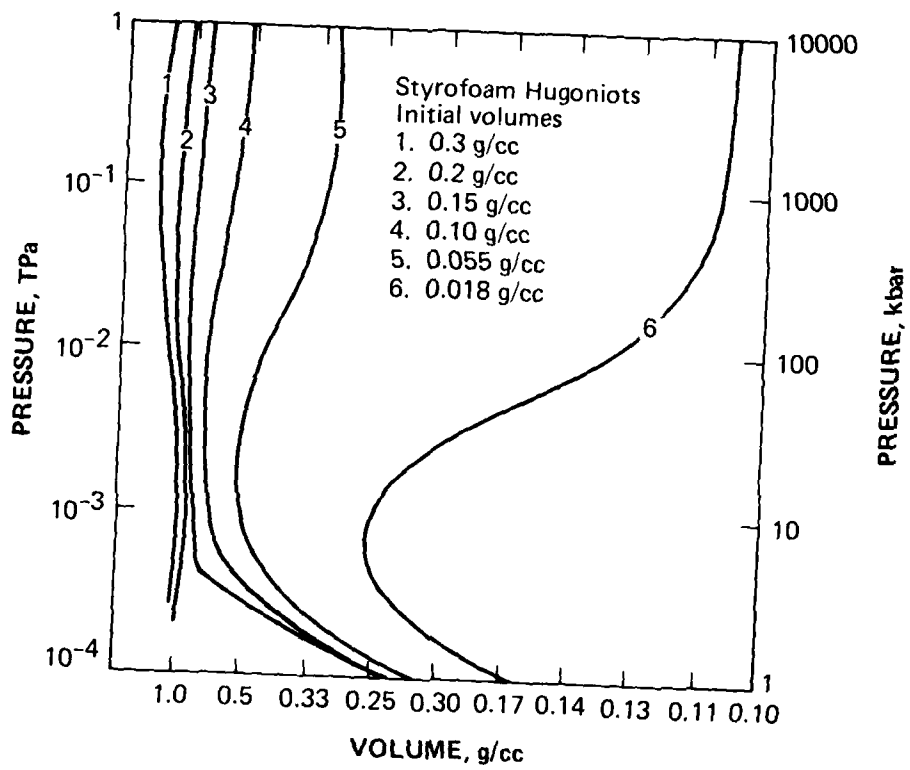


Figure 2.3 Dependence of theoretical styrofoam Hugoniots on initial volume (after Reference 12).

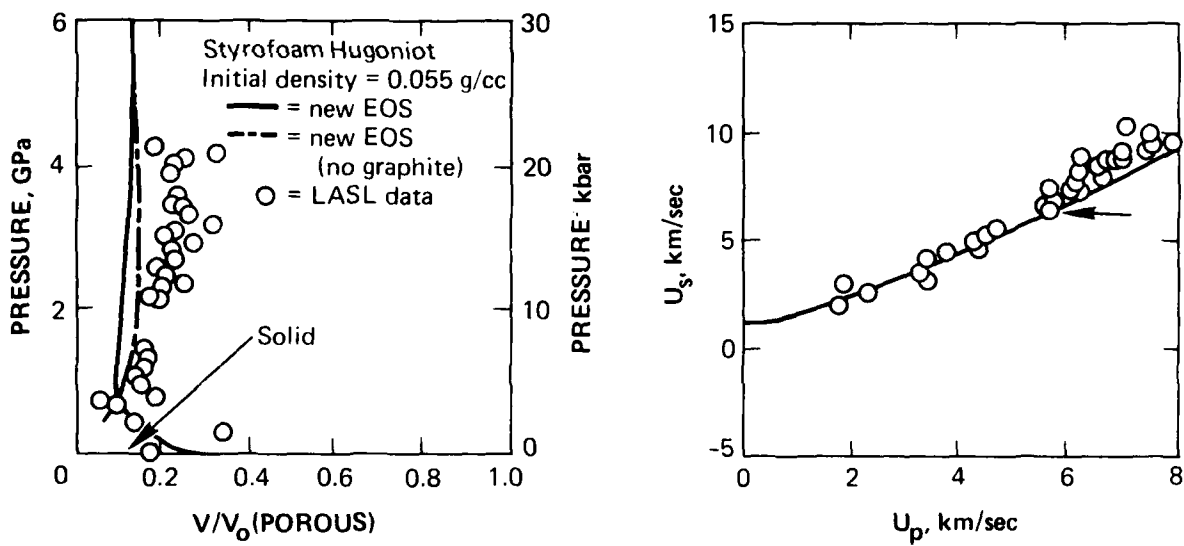


Figure 2.4 Styrofoam Hugoniot at initial density = 0.055 g/cc. Volume of (nonporous) solid polystyrene is indicated by arrow in the P vs. V/V_0 plot (after Reference 12).

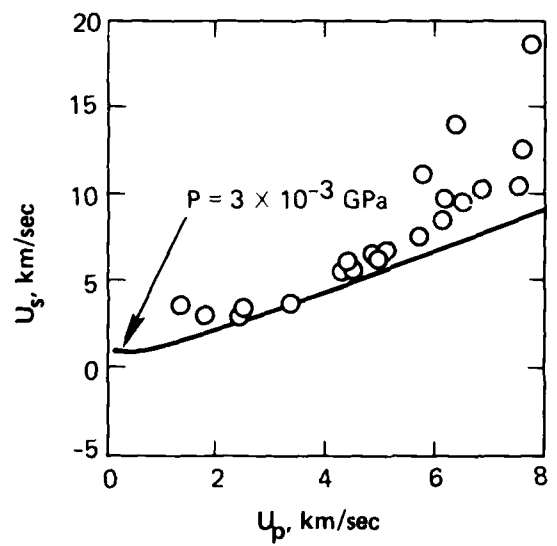
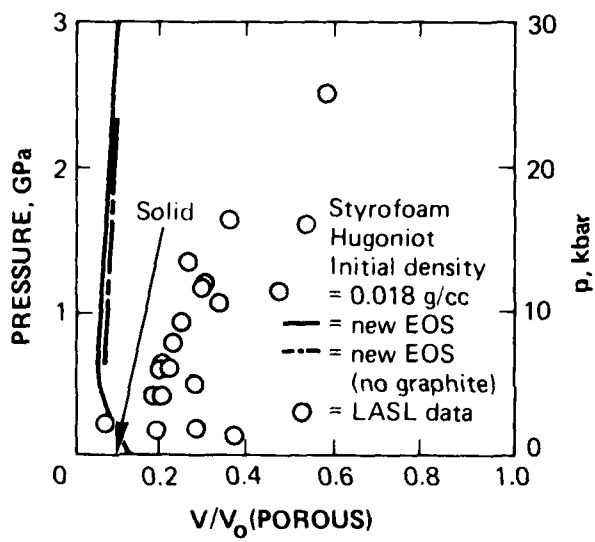


Figure 2.5 Styrofoam Hugoniot at initial density = 0.018 g/cc. Volume of (nonporous) solid polystyrene is indicated by arrow in the P vs. V/V_0 plot (after Reference 12).

$$P \text{ (Mbar)} = \frac{\rho_0 U_0^2 \mu (\mu + 1)}{[1 + \mu (1 + B)]^2} \quad (2.4)$$

where $\rho_0 = 0.54 \text{ g/cm}^3$
 $U_0 = 0.0481 \text{ cm}/\mu\text{s}$
 $B = 1.389$, and
 $\mu = \rho/\rho_0 - 1$.

Equation 2.4 is valid over a pressure range from 0.8 to 27.9 GPa (8 to 279 kbar), and thereby encompasses the Chapman-Jouguet (C-J) pressure of TNT (200 kbar).

Air was modeled using an ideal gas-type EOS (gamma-law) with the variable specific heat ratio found as a function of the air density and specific internal energy by table look-up (Reference 14). The initial air density was 0.001224 g/cm^3 .

SECTION 3

CALCULATIONAL RESULTS AND ANALYSES

One-dimensional (1D) calculations using PISCES 1DL and results obtained from previous two-dimensional (2D) calculations were used to assess the effects of: (1) differing high explosive models (Section 3.1), (2) reflecting versus soil ground surfaces (Section 3.2), and (3) inclusion of the charge support (Section 3.3), on the charge coupling for tangent-above 100 ton TNT spheres.

3.1 CONDITIONS WITHIN A 100 TON TNT SPHERE

One-dimensional calculations were used to compare conditions within the TNT sphere at the time that the detonation wave just reaches the edge of the 100 ton sphere, using the JWL and LSZK TNT models. The LSZK conditions, i.e., pressure P , specific internal energy, I , density, ρ , and velocity, V , are given in Reference 6. A 1D calculation was performed to obtain the corresponding JWL conditions. The results are summarized in Figures 3.1 to 3.4, respectively. The comparison is given at a time of 0.35 ms [the sphere radius is 2.405 m, and the TNT detonation velocity is 6.9 km/s (0.69 cm/ μ s)]. Close to the detonation front the comparison between the results of the two TNT models is quite good. Behind the front the JWL-calculated pressures and velocities are 10 to 20 percent lower than the LSZK-calculated values, but the densities and internal energies are slightly higher.

To investigate what effect these differences might have on charge coupling, a series of 1D calculations was performed. These employed spherical symmetry, and surrounded the TNT with soil, and with a rigid wall. Pressure versus time at the interface was monitored. The calculations were run to only 0.7 ms, and simulate (at best) only the conditions at the point of

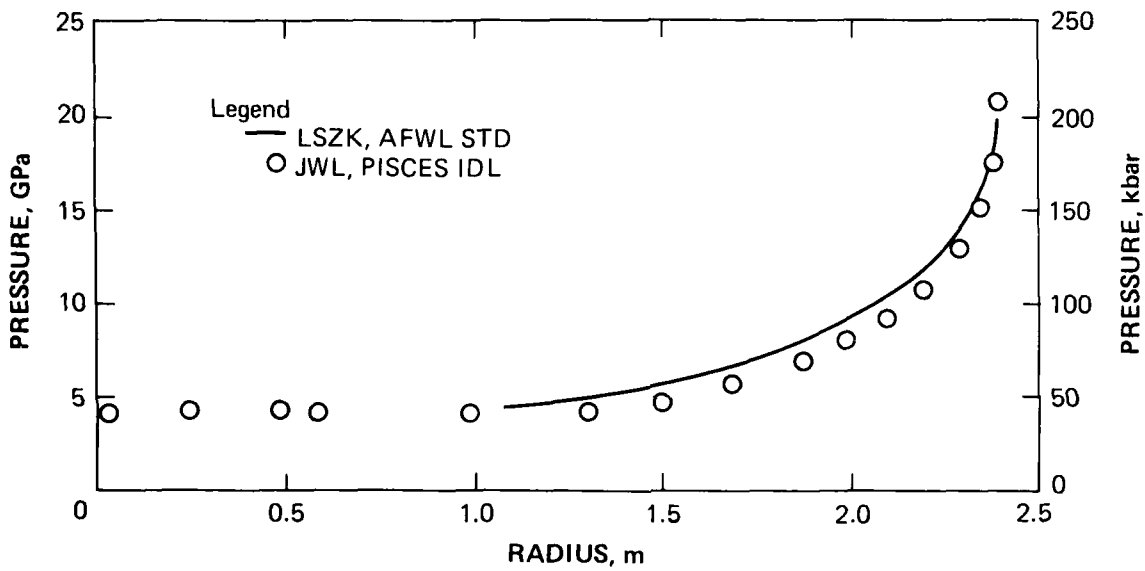


Figure 3.1 Pressure vs. radius within a 100 ton TNT sphere at a time all the explosive has detonated: a comparison using two different (LSZK and JWL) explosive equations of state.

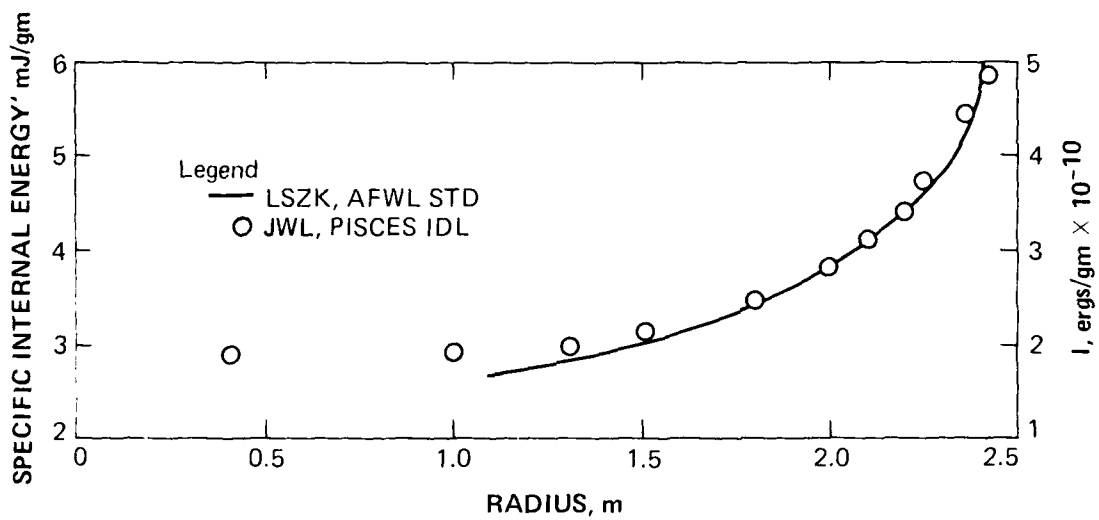


Figure 3.2 Specific internal energy vs. radius within a 100 ton TNT sphere at the time all the explosive has detonated: a comparison using two different (LSZK and JWL) explosive equations of state.

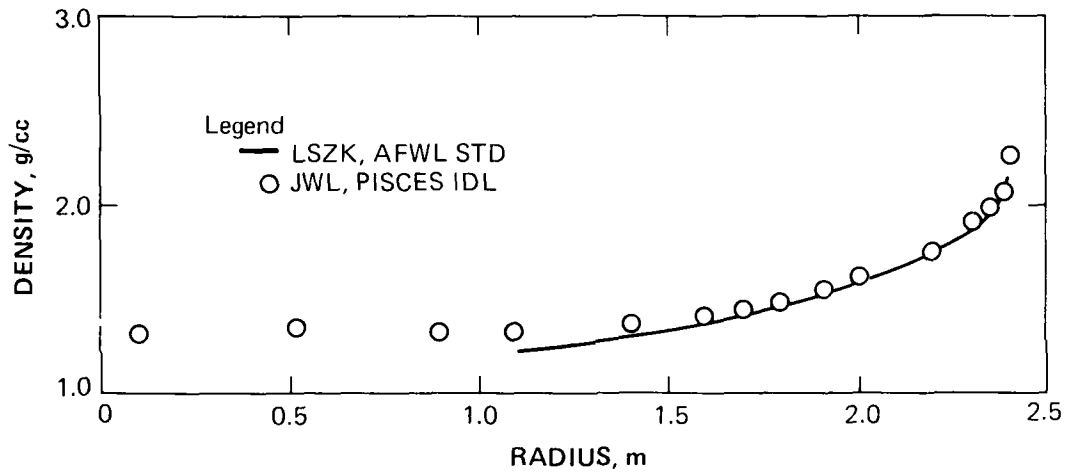


Figure 3.3 Density vs. radius within a 100 ton TNT sphere at the time all the explosive has detonated: a comparison using two different (LSZK and JWL) explosive equations of state.

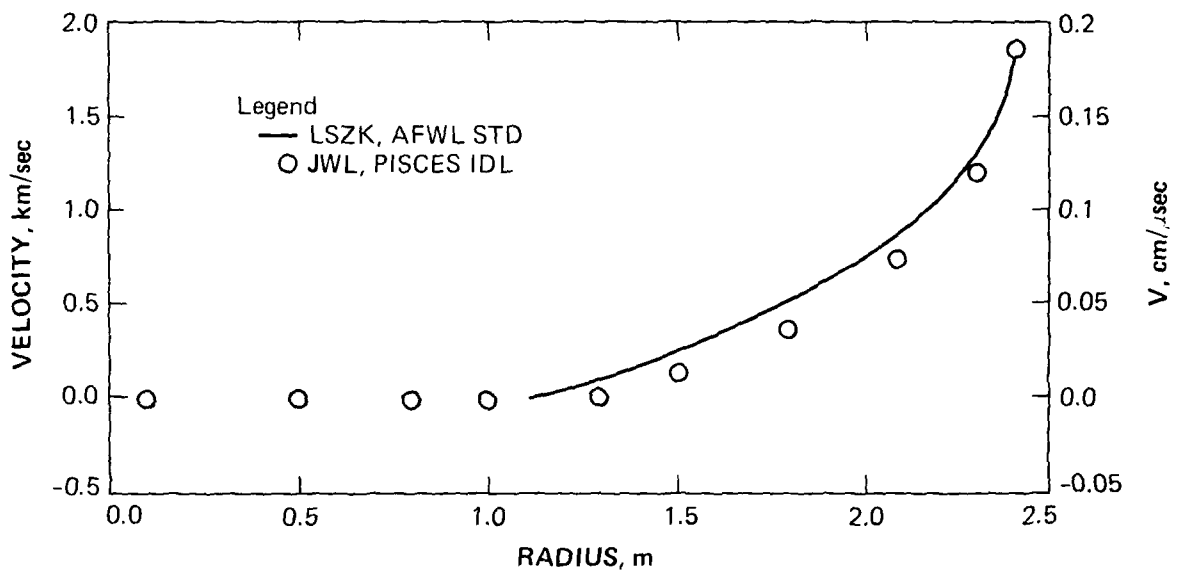


Figure 3.4 Particle velocity vs. radius within a 100 ton TNT sphere at the time all the explosive has detonated: a comparison using two different (LSZK and JWL) explosive equations of state.

tangency between the sphere and the surface. Actually, 2D effects are very important, and the results can be compared only in a relative sense. The results are shown in Figure 3.5, along with the 2D result from the AFWL recalculation of a 100 ton tangent-above TNT sphere (Reference 3). As expected, the JWL-calculated curve lies below the LSZK-calculated curve for both the soil and rigid wall calculations. This implies about a 13 percent lower total impulse for the JWL model. Two-dimensional effects are important throughout the coupling process, as seen by comparing these 1D results with the AFWL recalculation* (Reference 3). One can conclude that a 2D calculation using the JWL EOS with a rigid surface would produce a pressure-time curve that would lie below the AFWL LSZK points presented in Figure 3.5.

3.2 MODELING OF THE AIR-GROUND INTERFACE

This section reviews past 2D cratering calculations and the techniques used to model the air-ground interface. Any such discussion must begin with the AFWL airblast-only calculations performed for tangent-above TNT sphere events over the past 13 years. Pressure histories from these calculations have been used as boundary conditions for cratering calculations modeling many different site geologies. Table 3.1 summarizes pertinent information for three AFWL calculations: those of Nawrocki et al. for the 100 ton event Distant Plain 6 (Reference 6), Needham for the 500 ton Prairie Flat event (Reference 15), and Needham's unpublished recalculation of 100 ton event (Reference 3). All three of these calculations used the AFWL STD conditions for the completely detonated TNT sphere; the LSZK EOS to describe the detonation products, and a rigid ground surface. Stations at which the airblast overpressure histories were saved along the rigid surface are given for each calculation (stations from the Prairie Flat calculation were scaled to 100 tons using cube root

*The apparent agreement between the 2D AFWL recalculation and the 1D JWL/SOIL calculation is purely coincidental.

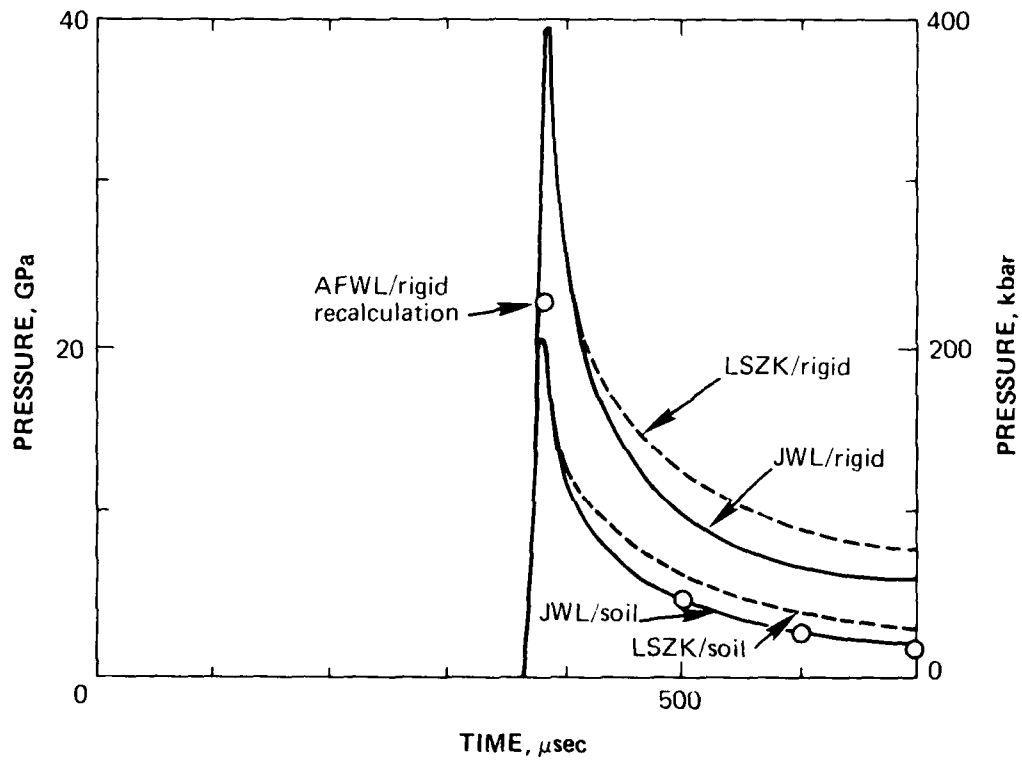


Figure 3.5 Pressure histories at the edge of a 100 ton TNT sphere from 10 calculations using the JWL and LSZK TNT equations of state (2D results from the AFWL recalculation (3) are denoted by circles).

Table 3.1 Summary of airblast calculations performed by AFWL for 100 to 500 ton spherical TNT charges tangent-above a rigid surface.

Calculator (first author)	Date	Associated Event	HE		Computer Code	Computer Close-in Ranges for P(t) Along Surface*	Report Number
			Type	Weight			
Nawrocki	1967	Distant Plain 6	TNT	100 tons	Shell-2	3.6 M (12 ft)	AFWL-TR-67-57 (Reference 6)
						4.6 M (15 ft)	
						6.4 M (21 ft)	
						7.6 M (25 ft)	
Needham	1969	Prairie Flat	TNT	500 tons	Shell-2	0.0 M (0 ft)	AFWL-TR-69-4 (Reference 15)
						4.3 M (14 ft)	
						5.0 M (16.4 ft)	
						6.6 M (21.6 ft)	
Needham	1978	--	TNT	100 tons	Hull	0.0 M (0 ft)	unpublished (Reference 3)
						0.6 M (2 ft)	
						1.2 M (4 ft)	
						2.1 M (7 ft)	
						3.0 M (10 ft)	

*Ranges scaled to 100 tons

scaling). One of the deficiencies of the 1967 and 1969 calculations was that overpressure and impulse histories were not saved along the surface over the TNT charge radius; this deficiency was corrected by the 1978 recalculation.

For the purposes of this discussion, the cratering calculations for surface tangent-above spherical HE events can be placed into two categories: those which included the HE source (Table 3.2) and those which used a pressure-time boundary condition to describe the surface loading (Table 3.3). It is useful to compare some results for the two types of calculations because such a comparison shows whether the pressure-time boundary condition is an adequate representation of the surface loading. Specific comparisons were made for total energy coupled to the ground, and total impulse versus range.

The maximum total coupled energy is summarized in Table 3.2 for the first class of cratering calculations. The Distant Plain 6 calculation clearly overestimates the coupled energy because of the extremely high value of gamma used to describe the entire source region. That reported for the pre-Mine Throw IV calculation is a clear underestimation for the reason given in the table footnote. Thus Table 3.2 yields only one relevant coupled energy number, the 5.6% reported for the Mixed Company III calculation (Reference 17).

A majority of the more recent calculations have used pressure-time boundary conditions, as indicated by Table 3.3. Most have been performed using a combination of the results from the Prairie Flat airblast calculation and Schuster's 1972 Middle Gust III calculation to define the boundary condition. Schuster's calculation (containing the HE source) is used to provide the first 1.1 ms (scaled) of the boundary condition; the calculated Prairie Flat airblast is used to describe later times. For a wide range of geologies, Table 3.3 indicates that the total coupled energy lies between 5 and 6.8 percent, in close agreement with the 5.6 percent reported by Ialongo (Table 3.2). This good agreement between the two approaches indicates that the pressure-

Table 3.2 Summary of aspects of the close-in coupling for calculations of target-above HE spheres in which the HE was included.

Calculator (first author)	Date	Event	Type	HIGH EXPLOSIVE				Percent of Total Energy Coupled to Ground	Site Geology	Report Number
				Weight	Detonation Model	Detonation Products Model	Charge Support Model			
Christensen	1968	Distant Plain 6	TNT	100 tons	Gamma- law (1)	Gamma- law (1)	Gamma- law (1)	7.3%	DRES soil Alluvium	DASA 2360 (Reference 16)
Ialongo	1973	Mixed Company III	TNT	500 tons	APWL STD	JWL	Low density soil (2)	5.6%	Sand over sandstone	DNA 3206T (Reference 17)
Borden	1976	Pre Mine Throw IV	NM (3)	100 tons	JWL	JWL	None (4)	4.2% (5)	Playa	DNA 4153F (Reference 18)
Schuster	1977	Middle Gust III (6)	TNT	100 tons	APWL STD	JWL	None	Not reported	Alluvium over sandstone	APWL-TR-76-284 (Reference 19)

- (1) HE, charge support, and air in one-material Eulerian grid, gamma = 2.727.
- (2) Initial density of support = 0.032 g/cm³, P = 0 until $\rho = 1.79$ g/cm³.
- (3) Nitromethane.
- (4) Reduced size charge support used in experiment.
- (5) Energy coupled to Lagrangian grid only, so total energy should be higher.
- (6) Calculation run to 1.1 ms to obtain pressure-time boundary condition for cratering calculation (for times ≤ 1.1 ms).

Table 3.3 Summary of the energy coupling for cratering calculations which used a pressure-time expression to describe the surface loading from 100 to 500 kt surface tangent-above TNT spheres.

Calculator (first author)	Date	Event	TNT Weight	P(t) Source	Percent of Total Energy Coupled to Ground	Site Geology	Report Number
Schuster	1977	Middle Gust III	100 tons	Scaled Prairie Flat, Needham, 1967, (1)	Not reported	Wet Alluvium over shale	AFWL-TR-76-284 (Reference 19)
Port	1973	Middle Gust III	100 tons	Scaled Prairie Flat, Needham, 1967, (1)	Not reported	Wet Alluvium over shale	DNA 3151 P2 (Reference 20)
Ullrich	1979	Multiple Aim Point (MAP) 5.2	500 kt	Scaled Prairie Flat, Needham, 1967, (1)	5.3%	Alluvium over dry rock (2)	AFWL-TR-78-189 (Reference 21)
Ullrich	1979	Map 5.2.1	500 tons	Prairie Flat, Needham, 1967, (1)	5.3%	Alluvium over dry rock, 1/10 scale site (2)	AFWL-TR-78-189 (Reference 21)
Dzwilewski	1979	Pre Dice Throw II-1	100 tons	Scaled Prairie Flat, Needham, 1967, (1)	6.8%	Alluvium over wet Alluvium	AFWL-TR-79-2 (Reference 22)
Dzwilewski	1979	Mixed Company III	500 tons	Prairie Flat, Needham, 1967, (1)	6%	Sand over sandstone	AFWL-TR-79-2 (Reference 22)
Schuster	1979	Middle Gust III	100 tons	Recommended fit	5%	Wet Alluvium over shale	Current effort

(1) First 1.1 scaled ms of P(t) from coupled HE-ground calculation by Schuster (scaled to appropriate yield).

(2) One-tenth scale of site geology is crudely similar to the Mixed Company III site.

time boundary condition is an acceptable way of defining the overall surface loading.

The boundary condition used in the current Middle Gust III baseline calculation differs from previous approaches (see introduction). Figure 3.6 compares the total coupled energy versus time from one of the preliminary (current) CRT calculations with that reported by Ialongo for Mixed Company III. Excellent agreement is seen within the first 2 to 3 scaled milliseconds; differences in site geology probably account for the differences at later times.

Finally, the close-in total impulse is compared (Figure 3.7) for the 1978 AFWL 100 ton sphere recalculation (Reference 3), Schuster's 1972 Middle Gust III calculation (Reference 23) and Needham's (scaled) Prairie Flat calculation (Reference 23). The first two agree very well; the latter is a linear interpolation between 0 and 4.3 scaled meters, which obviously overpredicts the impulse in this range. It can be concluded that the close-in boundary condition currently being used by CRT for the Middle Gust III cratering calculation is an acceptable representation of the direct surface loading from a 100 ton surface tangent-above TNT sphere without any charge support structure.

3.3 EFFECT OF THE CHARGE SUPPORT STRUCTURE

Previous cratering calculations were also reviewed with respect to the modeling of the charge support structure. The data base is limited to those calculations listed in Table 3.2. Of those, only one calculation actually attempted to model the structure, the Mixed Company III calculation of Ialongo (Reference 17). The model used, as described in the footnote in Table 3.2, did not allow for any resistance of the styrofoam to initial shock compression. More recent EOS models for styrofoam indicate that there is substantial resistance, caused by shock heating, if the initial density of the styrofoam is very low (as it is in the support structure). To see what effect a more realistic material model for styrofoam might have on the impulse

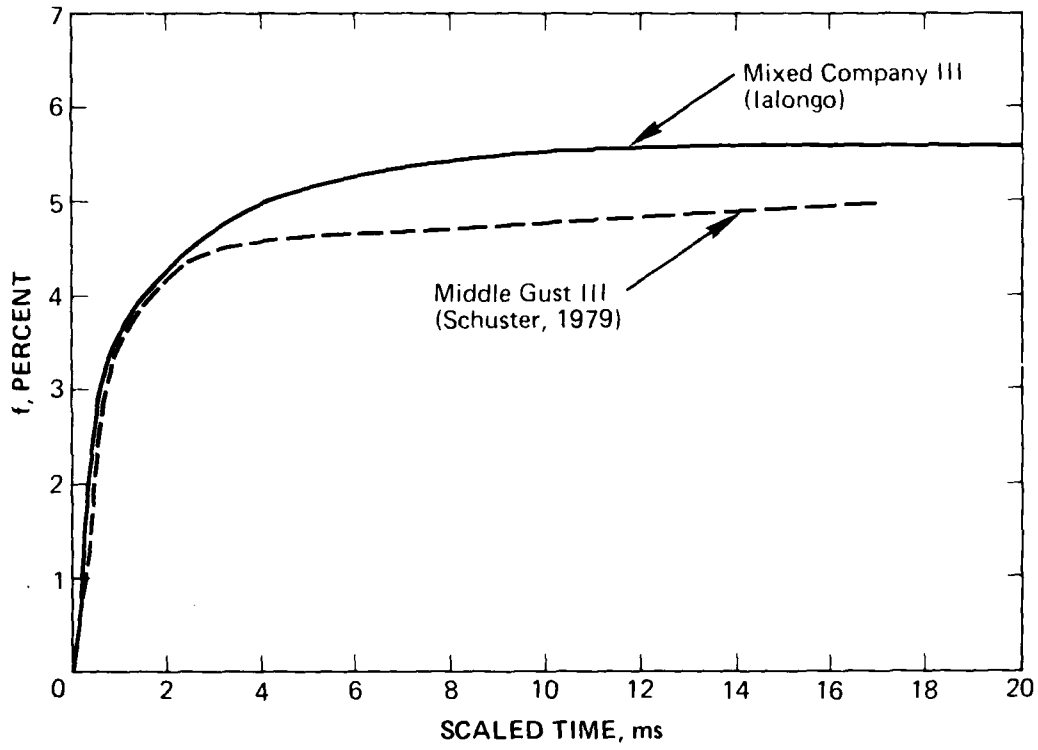


Figure 3.6 Percent of yield coupled to the ground versus time for the Mixed Company event (500 tons) and the Middle Gust III event (100 tons).

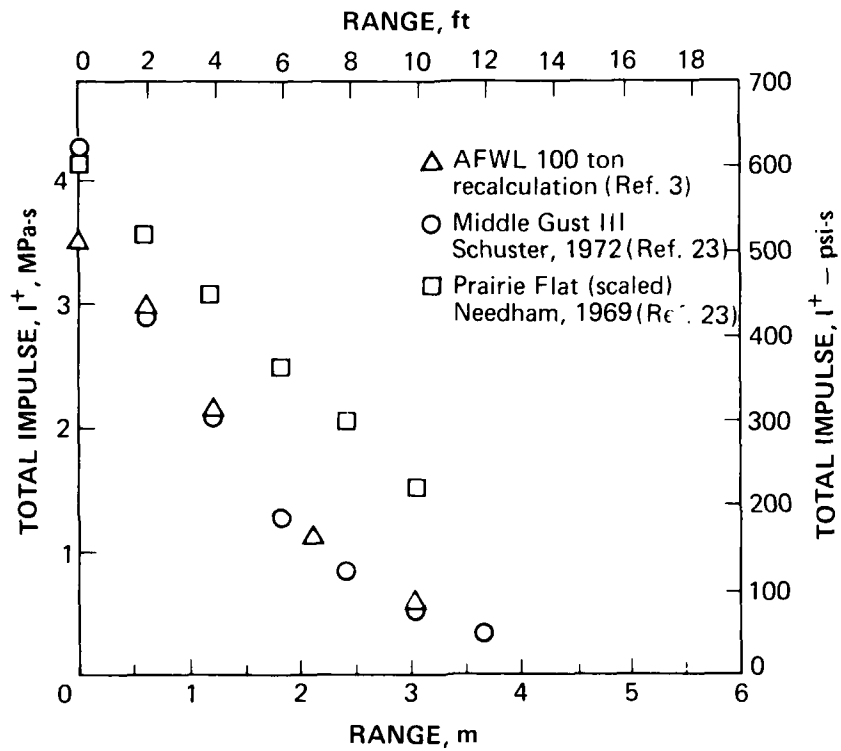


Figure 3.7 Comparison of close-in total impulse delivered to the ground by 100 ton surface tangent-above TNT spheres.

delivered to the soil, a series of 1D calculations was performed using the styrofoam EOS described in Section 2. The 100 ton TNT sphere was modeled using the LSZK EOS.

Calculations were performed for a surface range of 2.3 m (7.5 ft), corresponding to a radial distance between the edge of the TNT sphere and the ground surface of 0.93 m (3 ft). This is close to the maximum thickness of styrofoam between the edge of the charge and the ground surface in the Middle Gust III experiment. The space between the sphere and the Middle Gust soil (see Section 2) in the 1D (spherically symmetric) calculations was filled with air, styrofoam, and styrofoam with 38.1 mm (1½ in.) of plywood on top of the soil. Pressure and impulse were monitored at the soil "surface" and pressure was monitored at a depth of 0.5 m in the soil (soil was placed to a total depth of 5 m in the calculations).

It was found that the styrofoam absorbed about five times more energy than air; the absolute value for styrofoam was about 10 percent of the total energy. Figures 3.8 and 3.9 compare the pressure-time and impulse-time profiles from the 1D calculations, respectively. It is obvious that the plywood does not affect the results. The air-filled region allows the shock from the TNT sphere to arrive sooner (0.25 ms after the sphere is completely burned*) than the styrofoam does, but the initial pressure pulse is broader with the styrofoam (Figure 3.8). Total impulse (Figure 3.9) is about the same for both calculations after 0.3 ms. In the soil (Figure 3.10) the maximum pressure using styrofoam filler is higher than with air [4.2 GPa versus 2.2 GPa (42 versus 22 kbar)].

These results indicate only the general trend one could expect if the charge support structure were modeled in a 2D calculation. Although the total impulse delivered to the soil does not appear to be significantly affected by the presence of the

*All times are measured from the time the TNT sphere is totally burned.

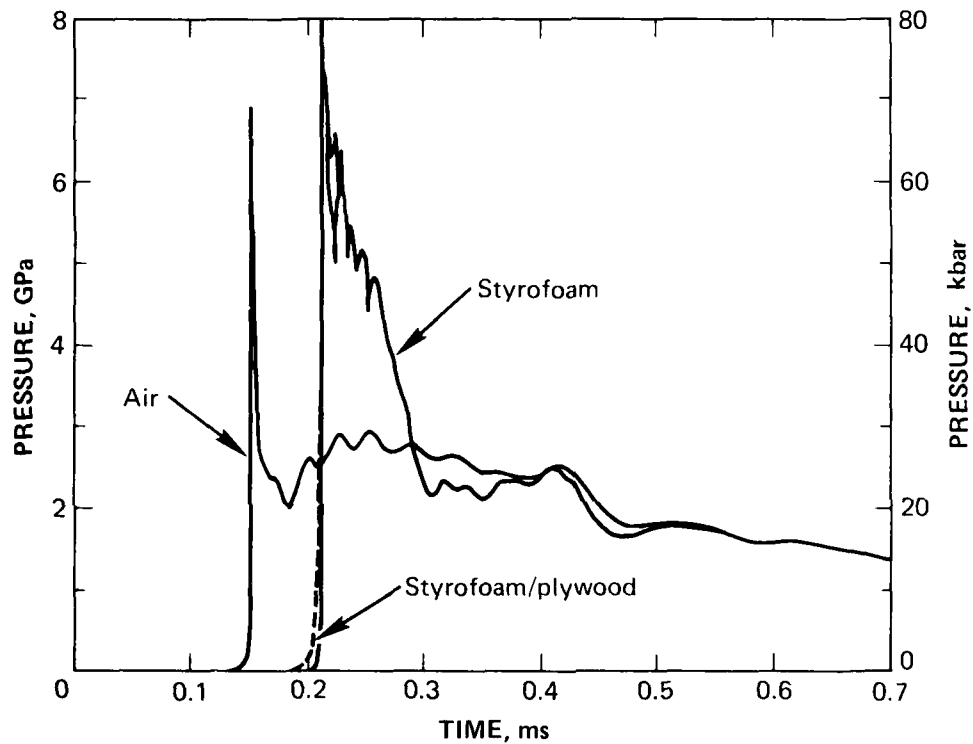


Figure 3.8 Pressure histories at the soil interface (1D calculations) corresponding to a surface range of 2.3 m (7.5 ft) from the point of tangency of a 100 ton TNT sphere.

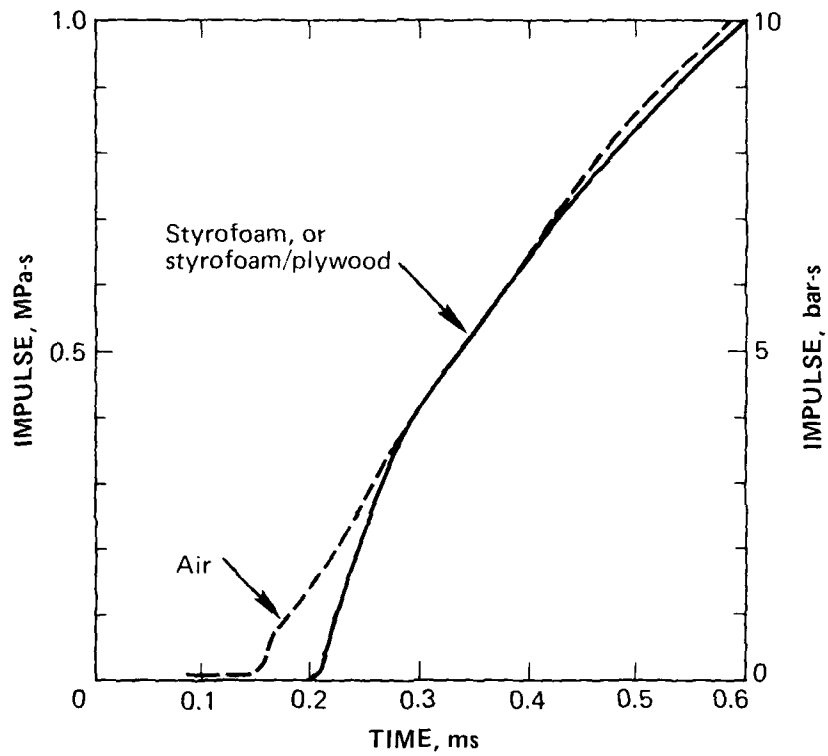


Figure 3.9 Specific impulse at the soil interface (1D calculations) corresponding to a surface range of 2.3 m (7.3 ft) from the point of tangency of a 100 ton TNT sphere.

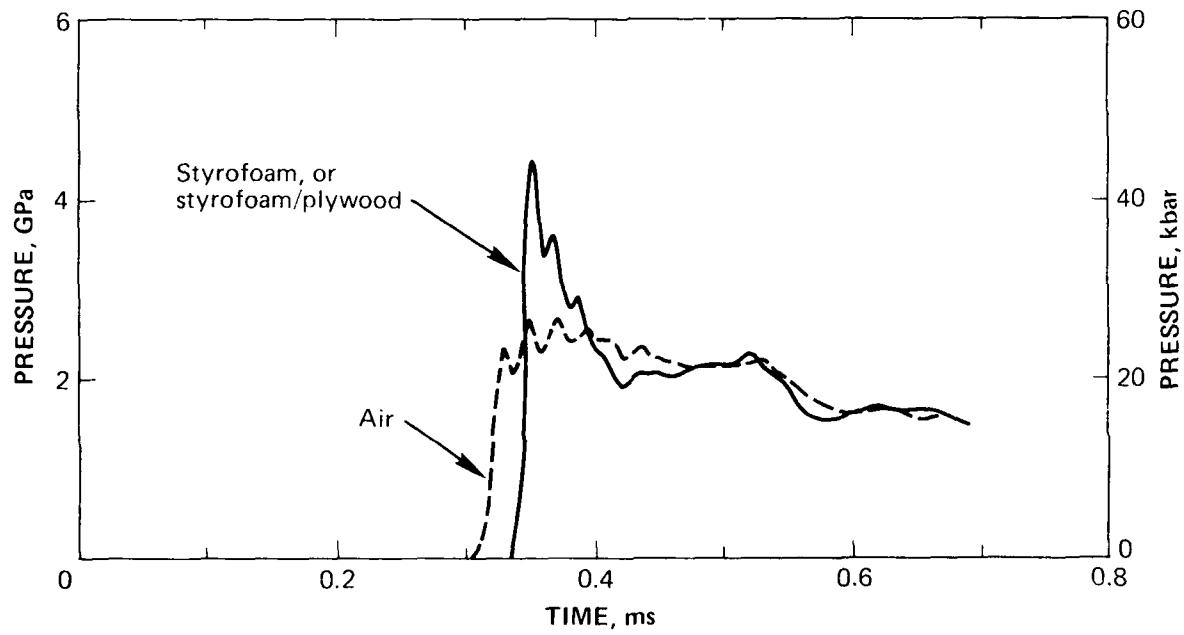


Figure 3.10 Pressure histories at a 0.5 m (1.6 ft) depth in the soil.

styrofoam support, the initial shock pressure seen at, and slightly below the soil surface may be up to a factor of two higher if the charge support were modeled better. The absolute effect of the structure on the initial coupling can only be determined by performing a 2D calculation.

SECTION 4

CONCLUSIONS

Calculational techniques used in prior surface-tangent TNT sphere cratering calculations were reviewed with respect to the modeling of the interaction of the TNT source with the ground. Three basic types of modeling have been used:

1. Start with the detonated TNT charge and allow it to interact with a realistic ground surface.
2. Start with a pressure-time boundary condition derived from AFWL airblast calculations which treat the surface as a reflecting boundary.
3. Hybrid Models - use the best parts of both (1) and (2).
 - a. Use a pressure-time boundary condition from (1) close-in, followed by one from (2) beyond 15 ft. Many AFWL cratering calculations, and the 1972 Middle Gust III (MGIII) cratering calculation, were performed this way.
 - b. Use a pressure-time boundary condition from (2) close-in, followed by a fit to event airblast data beyond 10 ft. This approach, which apparently has never been used before, is being used in the current CRT baseline MGIII cratering calculation.

A majority of the impulse and energy (≈ 80 percent) coupled to the ground is accomplished within the first 10 ft from the charge center. All approaches listed above give approximately the same total impulse at the ground surface over this range, and coupled energy. It can be concluded that the close-in surface loading model being used currently by CRT is an acceptable representation of the direct surface loading obtained from a 100 ton

surface tangent-above TNT sphere which has no support structure. None of the past cratering calculations has accurately modeled the charge support structure, which has consistently been a part of such experiments. The effect of this structure is probably to send a stronger shock into the ground initially, due to the resistance of styrofoam to the initial shock pressure. Total impulse delivered to the ground probably would not change significantly if the support structure were included, but since a 2D calculation has not been performed, this cannot be stated conclusively.

REFERENCES

1. L. S. Melzer, Recommended Blast Pressure Environment for the Middle Gust III Cratering Calculation, Civil Systems, Inc., Memo dated August 1, 1979.
2. J. Radler, Minutes of the Second Meeting of DNA Ad Hoc Cratering Working Group, RDA-TR-113204-003, R and D Associates, Marina Del Rey, CA, October 10-11, 1979.
3. R. J. Port, RDA memo dated 22 August 1979.
4. E. E. Jaramillo, Middle Gust III Free-Field Data Report, AL-831-3, EG&G, February 1, 1973.
5. F. Skinner, private communication, November 5, 1979.
6. E. A. Nawrocki, W. A. Whitaker, and C. E. Needham, Theoretical Calculations of the Phenomenology of Distant Plain, Event 6, AFWL TR-67-57, Air Force Weapons Laboratory, Kirtland AFB, NM, July 1967.
7. W. A. Whitaker, E. A. Nawrocki, C. E. Needham, and W. A. Troutman, Theoretical Calculations of the Phenomenology of HE Detonations, Volume I, AFWL TR-66-141, Air Force Weapons Laboratory, Kirtland AFB, NM, November 1966.
8. M. Lutzky, The Flow Field Behind a Spherical Detonation in TNT Using the Landau-Stanyukovich Equation of State for Detonation Products, NOLTR-64-40, U. S. Naval Ordnance Laboratory, MD, February 1965.
9. E. L. Lee, H. C. Hornig, and J. W. Kury, Adiabatic Expansion of High Explosive Detonation Products, Lawrence Livermore Laboratory, Livermore, CA, May, 1968.

10. J. S. Zelasko, MG III, Material Properties Studies and Calculations, in "Minutes of the First Meeting of DNA Ad Hoc Cratering Working Group," R & D Associates, Marina Del Rey, CA, June 7-8 1979.
11. M. F. Goodrich, J. B. Bryan, J. M. Thomsen, and C. M. Snell, Final Report on a Computational Parameter Study of Soils Typical of Some ESSEX I Cratering Sites, UCRL 52038, Lawrence Livermore Laboratory, Livermore, CA, March 1976.
12. F. H. Ree, Equation of State of Plastics: Polystyrene and its Foams, UCRL-51885, Lawrence Livermore Laboratory, Livermore, CA, August 1975.
13. J. Shaner, Los Alamos Scientific Laboratory, Los Alamos, New Mexico, private communication to J. Thomsen, June 1979.
14. PISCES 1DL Manual C, Non-Standard Options (Version 3), Physics International Company, San Leandro, CA.
15. C. E. Needham, Prairie Flat Airblast Calculations, AFWL 69-4, Air Force Weapons Laboratory, Kirtland AFB, NM, February 1969.
16. D. M. Christensen, C. S. Godfrey and D. E. Maxwell, Calculations and Model Experiments to Predict Crater Dimensions and Free-Field Motion, DASA 2360, September 1968.
17. G. Ialongo, Prediction Calculation for the Mixed Company III Event, DNA 3206T, November 1973.
18. F. Borden, R. Swift and D. Orphal, Pre-Mine Throw IV Cratering and Ground Motion Calculation, (unpublished).

19. S. Schuster, Results of Pre-Shot Prediction Calculations of Middle Gust I, II, and III, AFWL-TR-76-284, Air Force Weapons Laboratory, Kirtland AFB, NM, April 1977.
20. R. J. Port and R. Gajewski, "Sensitivity of Uniaxial Stress-Strain Relations on Calculations of Middle Gust Event III," Proceedings of the Mixed Company/Middle Gust Results Meeting, DNA 3151P2, March 13-15, 1973, May 1973.
21. G. W. Ullrich, Multiple Aim Point Ground Shock Environment Definition, AFWL-TR-78-189, Air Force Weapons Laboratory, Kirtland AFB, NM, July 1979.
22. P. T. Dzwilewski and G. W. Ullrich, Numerical Solution of the Cratering and Ground Shock From Actual High Explosive and Nuclear Tests, AFWL-TR-79-2, Air Force Weapons Laboratory, Kirtland AFB, NM, November 1978.
23. P. T. Dzwilewski, private communication to J. M. Thomsen, February 1980.

DISTRIBUTION LIST

DEPARTMENT OF DEFENSE

Assistant to the Secretary of Defense
Atomic Energy
ATTN: Executive Assistant

Defense Advanced Rsch Proj Agency
ATTN: TIO

Defense Intelligence Agency
ATTN: DB-4C, E. O'Farrell
ATTN: DT-1C
ATTN: DB-4N

Defense Nuclear Agency
2 cy ATTN: SPSS
4 cy ATTN: TITL

Defense Technical Information Center
12 cy ATTN: DD

Field Command
Defense Nuclear Agency
ATTN: FCTK
ATTN: FCPR

Field Command
Defense Nuclear Agency
ATTN: FCPRL

Interservice Nuclear Weapons School
ATTN: TTV

Joint Strat Tgt Planning Staff
ATTN: JLA
ATTN: NRI-STINFO Library

NATO School (SHAPE)
ATTN: U.S. Documents Officer

Undersecretary of Def for Rsch & Engrg
ATTN: Strategic & Space Systems (OS)

DEPARTMENT OF THE ARMY

BMD Advanced Technology Center
Department of the Army
ATTN: ATC-T
ATTN: 1CRDABH-X

Chief of Engineers
Department of the Army
ATTN: DAEN-RDM
ATTN: DAEN-MCE-D

Harry Diamond Laboratories
Department of the Army
ATTN: DELHD-N-P
ATTN: 00100 Commander/Tech Dir/TSO

U.S. Army Ballistic Research Labs
ATTN: DRDAR-BLT, W. Taylor
ATTN: DRDAR-TSB-S
ATTN: DRDAR-BLV
ATTN: DRDAR-BLE, J. Keefer

DEPARTMENT OF THE ARMY (Continued)

U.S. Army Concepts Analysis Agency
ATTN: CSSA-ADL

U.S. Army Engineer Center
ATTN: DT-LRC

U.S. Army Engineer Div Huntsville
ATTN: HNDED-SR

U.S. Army Engineer Div Ohio River
ATTN: ORDAS-L

U.S. Army Engr Waterways Exper Station
ATTN: WESSA, W. Flathau
ATTN: Library
ATTN: WESSD, J. Jackson
ATTN: J. Strange
ATTN: WESSE, L. Ingram

U.S. Army Material & Mechanics Rsch Ctr
ATTN: Technical Library

U.S. Army Materiel Dev & Readiness Cmd
ATTN: DRXAM-TL

U.S. Army Missile Command
ATTN: RSIC

U.S. Army Nuclear & Chemical Agency
ATTN: Library

DEPARTMENT OF THE NAVY

David Taylor Naval Ship R&D Ctr
ATTN: Code L42-3

Naval Construction Battalion Center
ATTN: Code LOBA
ATTN: Code L51, S. Takahashi

Naval Electronic Systems Command
ATTN: PME 117-21

Naval Facilities Engineering Command
ATTN: Code O3T
ATTN: Code O4B
ATTN: Code O9M22C

Naval Material Command
ATTN: MAT 08T-22

Naval Postgraduate School
ATTN: Code O142 Library

Naval Research Laboratory
ATTN: Code 2627

Naval Sea Systems Command
ATTN: SEA-09G53

Naval Surface Weapons Center
ATTN: Code F31

DEPARTMENT OF THE NAVY (Continued)

Naval Surface Weapons Center
ATTN: Tech Library & Info Svcs Branch

Naval War College
ATTN: Code E-11

Naval Weapons Evaluation Facility
ATTN: Code 10

Office of Naval Research
ATTN: Code 715
ATTN: Code 474, N. Perrone

Office of the Chief of Naval Operations
ATTN: OP 981
ATTN: OP 03EG

Strategic Systems Project Office
Department of the Navy
ATTN: NSP-43

DEPARTMENT OF THE AIR FORCE

Air Force Institute of Technology
ATTN: Library

Air Force Systems Command
ATTN: DLW

Air Force Weapons Laboratory
Air Force Systems Command
ATTN: NTE, M. Plamondon
ATTN: DYT
ATTN: NTES-C, R. Henny
ATTN: SUL

Assistant Chief of Staff
Intelligence
Department of the Air Force
ATTN: INT

Ballistic Missile Office
Air Force Systems Command
ATTN: MMH

Deputy Chief of Staff
Research, Development, & Acq
Department of the Air Force
ATTN: AFROQSM

Deputy Chief of Staff
Logistics & Engineering
Department of the Air Force
ATTN: LEEE

Foreign Technology Division
Air Force Systems Command
ATTN: NIIS Library

Rome Air Development Center
Air Force Systems Command
ATTN: TSLD

Strategic Air Command
Department of the Air Force
ATTN: NRI-STINFO Library

DEPARTMENT OF ENERGY

Department of Energy
Albuquerque Operations Office
ATTN: CTID

Department of Energy
Nevada Operations Office
ATTN: Mail & Records for Tech Lib

DEPARTMENT OF ENERGY CONTRACTORS

Lawrence Livermore National Laboratory
ATTN: W. Crowley
ATTN: L-10, H. Kruger
ATTN: J. Nutt
ATTN: Tech Information Dept Library

Los Alamos National Scientific Laboratory
ATTN: MS 362 Librarian
ATTN: M. Henderson
ATTN: G. Spillman
ATTN: MS 364
ATTN: R. Bridwell
ATTN: MS 670, J. Hopkins

Oak Ridge National Laboratory
ATTN: Civil Def Res Proj
ATTN: Central Research Library

Sandia National Laboratories
ATTN: Library & Security Class Div

Sandia National Laboratories
ATTN: A. Chabai
ATTN: 3141

OTHER GOVERNMENT

Central Intelligence Agency
ATTN: OSWR/NED

Department of the Interior
Bureau of Mines
ATTN: Tech Lib

Federal Emergency Management Agency
ATTN: Hazard Eval & Vul Red Div

DEPARTMENT OF DEFENSE CONTRACTORS

Acurex Corp
ATTN: J. Stockton

Aerospace Corp
ATTN: Technical Information Svcs

Agbabian Associates
ATTN: M. Agbabian

Applied Theory, Inc
2 cy ATTN: J. Trulio

AVCO Research & Systems Group
ATTN: Library A830

DEPARTMENT OF DEFENSE CONTRACTORS (Continued)

BDM Corp
ATTN: Corporate Library
ATTN: T. Neighbors

Boeing Co
ATTN: R. Schmidt
ATTN: Aerospace Library

California Research & Technology, Inc
ATTN: S. Schuster
ATTN: Library
ATTN: K. Kreyenhagen

California Research & Technology, Inc
ATTN: D. Orphal

Calspan Corp
ATTN: Library

University of Denver
Colorado Seminary
Denver Research Institute
ATTN: J. Wisotski

EG&G Washington Analytical Services Center, Inc
ATTN: Library

Eric H. Wang
Civil Engineering Rsch Fac
University of New Mexico
ATTN: N. Baum

Gard, Inc
ATTN: G. Neidhardt

General Electric Company—TEMPO
ATTN: DASIAC

IIT Research Institute
ATTN: Documents Library

Institute for Defense Analyses
ATTN: Classified Library

Kaman AvIDyne
ATTN: Library

Kaman Sciences Corp
ATTN: Library

Lockheed Missiles & Space Co, Inc
ATTN: Technical Information Center
ATTN: T. Geers

Lockheed Missiles & Space Co, Inc
ATTN: TIC-Library

McDonnell Douglas Corp
ATTN: R. Halprin

Merritt CASES, Inc
ATTN: Library
ATTN: J. Merritt

Nathan M. Newmark Consult Eng Svcs
ATTN: N. Newmark

Pacific-Sierra Research Corp
ATTN: H. Brode

DEPARTMENT OF DEFENSE CONTRACTORS (Continued)

Pacifica Technology
ATTN: Tech Library

Physics International Co
ATTN: J. Thomsen
ATTN: Technical Library
ATTN: L. Behrmann
ATTN: E. Moore
ATTN: F. Sauer

R & D Associates
ATTN: R. Port
ATTN: Technical Information Center
ATTN: J. Lewis
ATTN: J. Carpenter
ATTN: W. Wright, Jr
ATTN: C. MacDonald
ATTN: P. Haas

Science Applications, Inc
ATTN: Technical Library
ATTN: H. Wilson

Science Applications, Inc
ATTN: D. Bernstein
ATTN: D. Maxwell

Science Applications, Inc
ATTN: W. Layson

Southwest Research Institute
ATTN: W. Baker
ATTN: A. Wenzel

SRI International
ATTN: G. Abrahamson

Systems, Science & Software, Inc
ATTN: D. Grine
ATTN: T. Cherry
ATTN: K. Pyatt
ATTN: Library
ATTN: T. Riney
ATTN: R. Lafrenz

Terra Tek, Inc
ATTN: S. Green
ATTN: Library

Tetra Tech, Inc
ATTN: Library
ATTN: L. Hwang

TRW Defense & Space Sys Group
ATTN: Technical Information Center
ATTN: I. Alber
ATTN: D. Baer
ATTN: R. Plebuch
2 cy ATTN: N. Lipner

TRW Defense & Space Sys Group
ATTN: E. Wong
ATTN: P. Dai

Universal Analytics, Inc
ATTN: E. Field

DEPARTMENT OF DEFENSE CONTRACTORS (Continued)

Weidlinger Assoc, Consulting Engineers
ATTN: J. Isenberg

Westinghouse Electric Corp
ATTN: W. Volz

DEPARTMENT OF DEFENSE CONTRACTORS (Continued)

Weidlinger Assoc, Consulting Engineers
ATTN: J. Wright
ATTN: M. Baron

END

DATE
FILMED

1-81

DTIC